DOI: 10.13009/EUCASS2017-268

Numerical Simulation of a Boron Loaded Gel Fuel Ramjet Combustor

David Diskin and Benveniste Natan**
** Faculty of Aerospace Engineering*
Technion - Israel Institute of Technology, Haifa 3200003, Israel

Abstract
The flowfield in a boron loaded gel fuel ramjet combustor has been investigated. A theoretical model of the combustor, which considers the pulsatile combustion of the gel fuel droplets in combination with the boron particles ignition and combustion stages has been developed. The model has been solved numerically using the CFD code FLUENT and user defined functions, which models the boron ignition and combustion processes. Gelled kerosene droplets and boron particles were injected discretely to the burner flowfield. The combustor consists of a main air inlet and a bypass inlet. The cold air from the bypass inlet cause condensation of the boron oxide, thus exploiting latent heat and completing combustion.

Nomenclature

A_r = reaction rate constant
B = boron
c = mass concentration
c_p = heat capacity
C_D = drag coefficient
C = constant
$C_{r,j}$ = molar concentration reaction
D = diffusion coefficient
d = droplet diameter
E = energy
E_r = reaction activation energy.
k_G = source of turbulent kinetic energy due to velocity gradient
H = hydrogen
H_{vap} = latent heat of vaporization
h_{gas} = heat transfer coefficient
h = enthalpy
$h_{i,f}$ = enthalpy of formation
J_i = mass flow of chemical species i
k = thermal conductivity
k = turbulent kinetic energy
$k_{f,r}$ = reaction rate
m = total mass of the droplet
M = molecular weight
Nu = Nusselt Number
O = oxygen
p = pressure

Copyright © 2015 by David Diskin and Benveniste Natan. Published by the EUCASS association with permission.

DOI: 10.13009/EUCASS2017-268

Pr = Prandtl number
$\dot{Q}$ = heat rate
r_d = gel droplet radius
R = molar consumption rate
R_E = molar evaporation rate
$\Re_i$ = total generation rate of species i
R_i = generation rate of species i resulting from the chemical reaction
R_r = reaction
r = radial coordinate
S = chemical species generation rate resulting from evaporation or condensation
S_b - = stoichiometric mass ratio
S_h = heat addition/loss
S_i = generation rate of species *i* resulting from evaporation or condensation
S_m = mass source/sink
Sc_t = Schmidt number
T = temperature
t = time
u = x velocity
v = y velocity
w = z velocity
X = molar fraction
Y = mass fraction
Y_M = kinetic turbulent energy sink due to density change.

Greek

ε = turbulent dissipation
μ = viscosity
ν = stoichiometric coefficient for reactant/products
ρ = density
σ = Lennard-Jones constant collision diameter
σ = tensile stress
σ_{yield} = yield stress
σ_k = turbulent Prandtl number for k
σ_ε = turbulent Prandtl number for ε
Ω_μ = Lennard-Jones function collision integral.

Subscripts

D = droplet
B = boron
f = liquid fuel
g = gellant
fg = liquid fuel / gellant mixture
l = laminar

DOI: 10.13009/EUCASS2017-268

1. Introduction

The ramjet engine is an air breathing propulsion means, which relies on the ram effect for compressing the entering air, thus, eliminating the need of a compressor. Therefore, ramjets have no moving parts and the working regime is suited for higher velocity compared to turbojets. The entering air is compressed in a unique diffuser through series of shocks, then, the air is mixed with fuel and ignited. Finally, the burned gases accelerate in a converging-diverging nozzle and thus generating thrust. The main disadvantage of the ramjet is the requirement to be accelerated by a rocket booster to the point where air compression is sufficient for the ram effect to take place. A review on the progression in the 20 century and various types of ramjet engines is described by Fry [1].
Metalized gel fuel used in ramjet engine has potential for higher performance and increased safety in comparison to the conventional Liquid Fuel Ramjets, Solid Fuel Ramjets or Ducted Rockets [2]. Gel propellants are liquid fuels or oxidizers, whose rheological properties have been altered by the addition of gelling agents. The gel is defined as “a substance that contains a continuous solid skeleton enclosing a continuous liquid phase. The continuity of the solid structure gives elasticity to the gel”. From the fluid mechanics point of view, gels behave as time dependent, non-Newtonian fluids. These properties enable to inject the gel similarly to liquids. Furthermore, its structure enables the addition of metal particles to the gel fuel. The motivation for the development of gel propellants originates from the significantly higher energetic performance of metalized fuels in bipropellant systems in comparison to non-metalized, hydrocarbon fuels. The existence of yield strength in gels, in combination with their high viscosity, allows the addition of high-energy metal particulates without sedimentation. However, gel propellants, since their viscosity varies with changing shear rate and in some cases even under constant shear rate, require designated atomization systems, characterized by higher pressure gradients than in liquid atomizers. Moreover, they require lack of stagnation points in the ejector in order to avoid accumulation of gel. The main disadvantage of gel fuels is the relatively low burning rates in comparison to liquid fuel droplets. In addition, possible, although limited, phase separation and physical instabilities during storage or acceleration may exist.
Boron is a metal with the highest volumetric specific energy in the nature, as shown in figure 1. As the early study of Haddad et al. [2] showed the high-performance potential of a boron loaded ramjet engine with specific impulse higher than 2000 s.

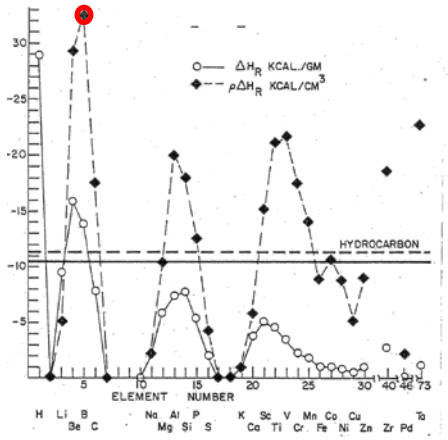

Figure 1: Specific energy of chosen elements

The ignition and combustion behavior of boron-containing propellants is very complex [3]. Boron particles are covered with a thin layer of boron oxide, which prevents oxidation of the boron particle. As a result, we can define two steps for the combustion of the particle: the first stage comprises the particle heating and the removal of the oxide layer exhibiting a weak glowing. This period is relatively long and usually denoted as ignition delay time. As soon as the oxide layer is removed, the ‘‘clean” boron particle burns vigorously and glows brightly, since then, the oxygen can reach the particle surface unrestricted. This second period is denoted as particle combustion time. The boron particle combustion is based on d^2-law. Boron combustion is inefficient at high fuel/air ratios since less oxygen is available for complete combustion [4]. Moreover, in order to exploit the energetic potential of boron, boron oxide needs to condense in order to release the evaporation latent heat; therefore, bypass air is required for completing boron combustion and condensation of the oxide.
The main objective of the study presented in this paper is to conduct a parametric investigation of the effect of boron concentration, boron particles diameter and size distribution, and bypass air ratio on the performance of the ramjet.
In the following sections, we will explain the assumptions underlying the computational and theoretical models, describe the model governing equations and the boundary conditions, the method of solution.

DOI: 10.13009/EUCASS2017-268

2. Problem Description and Mathematical Model

A three-dimensional ramjet combustor was modelled and solved using a commercial CFD software code (FLUENT). The combustor includes a long combustion chamber, fuel injectors, V shape flame stabilizers, bypass air inlet and a nozzle with convergence and divergence angles of 30° and 15° respectively. The boundary conditions upstream the combustor were defined using 1-D calculation of a non-ideal ramjet diffuser. The throat and nozzle exit areas were calculated from 1-D flow assuming an adapted to the ambient pressure nozzle. The model dimensions, gelled kerosene fuel droplet injection, boron particle injections location and model properties are described in Fig. 2. The gelled kerosene fuel droplet was modelled as a liquid droplet except that its evaporation pressure, which controls the rate of vaporization, was altered to be a function of time to describe oscillatory evaporation of the gel droplet and the droplet boiling temperature was altered to 600 K (gel evaporation temperature) [5]. The boron particles were modelled as injected downstream of the kerosene injection, where the particle separates from the droplet.

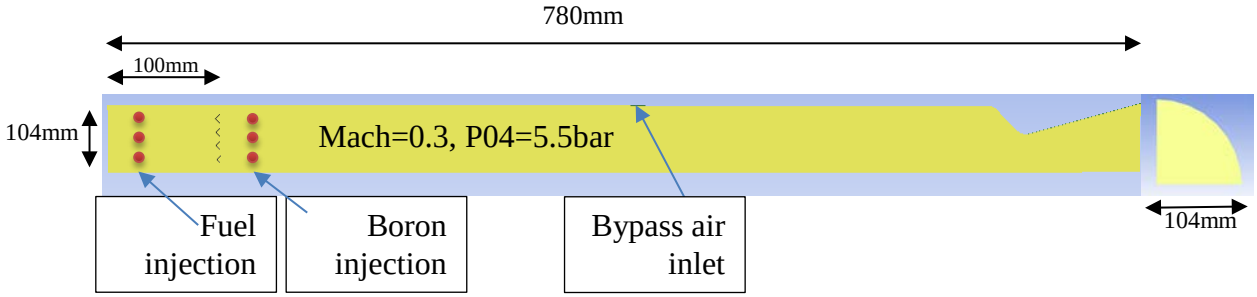

Figure 2. Modelled Ramjet combustor dimensions and properties

The mathematical model considers a three-dimensional geometry. Also assumes that the liquid volume is relatively small compared to the gas volume. Gravity force and heat transition by radiation are neglected. The governing equations of the combustor model are described in the following section.
Continuity equation:

$$\frac{\partial}{\partial x}(\rho u)+\frac{\partial}{\partial y}(\rho v)+\frac{\partial}{\partial z}(\rho w)=S_m \tag{1}$$

Momentum conservation in x, y and z directions:

$$\begin{aligned}
&\rho\left(u\frac{\partial u}{\partial x}+v\frac{\partial u}{\partial y}+w\frac{\partial u}{\partial z}\right)=-\frac{\partial p}{\partial x}+\frac{\partial}{\partial x}\left[2\mu\frac{\partial u}{\partial x}+\lambda\nabla\cdot\vec{V}\right]+\frac{\partial}{\partial y}\left[\mu\left(\frac{\partial u}{\partial y}+\frac{\partial v}{\partial x}\right)\right]+\\
&+\frac{\partial}{\partial z}\left[\mu\left(\frac{\partial w}{\partial x}+\frac{\partial u}{\partial z}\right)\right]\\
&\rho\left(u\frac{\partial v}{\partial x}+v\frac{\partial v}{\partial y}+w\frac{\partial v}{\partial z}\right)=-\frac{\partial p}{\partial y}+\frac{\partial}{\partial y}\left[2\mu\frac{\partial v}{\partial y}+\lambda\nabla\cdot\vec{V}\right]+\frac{\partial}{\partial z}\left[\mu\left(\frac{\partial v}{\partial z}+\frac{\partial w}{\partial y}\right)\right]+\\
&+\frac{\partial}{\partial x}\left[\mu\left(\frac{\partial u}{\partial y}+\frac{\partial v}{\partial x}\right)\right]\\
&\rho\left(u\frac{\partial w}{\partial x}+v\frac{\partial w}{\partial y}+w\frac{\partial w}{\partial z}\right)=-\frac{\partial p}{\partial z}+\frac{\partial}{\partial z}\left[2\mu\frac{\partial w}{\partial z}+\lambda\nabla\cdot\vec{V}\right]+\frac{\partial}{\partial x}\left[\mu\left(\frac{\partial w}{\partial x}+\frac{\partial u}{\partial z}\right)\right]+\\
&+\frac{\partial}{\partial y}\left[\mu\left(\frac{\partial v}{\partial z}+\frac{\partial w}{\partial y}\right)\right]
\end{aligned} \tag{2}$$

where the turbulence added to the momentum equations as turbulent viscosity: $\mu=\mu_l+\mu_t$
Energy equations:

$$\nabla\cdot(\vec{V}(\rho E+p))=\nabla\cdot\left(k\nabla T-\sum_i h_i\vec{J}_i\right)+S_h \tag{3}$$

DOI: 10.13009/EUCASS2017-268

$$E = h - \frac{p}{\rho} + \frac{u^2 + v^2 + w^2}{2} \tag{4}$$

The heat source S_h in the energy equation is heat loss due to droplet evaporation and heat addition due to chemical reaction:

$$S_h = -\sum_i \frac{h_i^0}{M_i} R_i \tag{5}$$

where h_i^0 is the enthalpy of formation and R_i is the total generation rate of the chemical i species.
Chemical species conservation equation:

$$\rho\left(u\frac{\partial Y_i}{\partial x} + v\frac{\partial Y_i}{\partial y} + w\frac{\partial Y_i}{\partial z} \right) = -\left[\frac{\partial J_{ix}}{\partial x} + \frac{\partial J_{iy}}{\partial y} + \frac{\partial J_{iz}}{\partial z} \right] + R_i + S_i \tag{6}$$

where R_i is the generation rate of the chemical species i resulting from the chemical reaction and S_i is the generation rate resulting from the evaporation or condensation of the liquid or gas phase respectively. J_{ix}, J_{iy}, J_{iz} are the diffusive mass fluxes of chemical species i in x, y and z directions respectively.
The mass flux of the chemical species due to J_i concentration gradient is given by:

$$\vec{J}_i = -\rho\left(D_{i,m} + \frac{\mu_t}{Sc_t} \right) \nabla Y_i \tag{7}$$

where Sc_t is turbulent Schmidt number and given by:

$$Sc_t = \frac{\mu_t}{\rho D_t} \tag{8}$$

Y_i is mass fraction of species i, $D_{i,m}$ is diffusion coefficient of chemical species i in the mixture, μ_t is turbulent viscosity and D_t is turbulent diffusion coefficient. The laminar viscosity is calculated according to the kinetic theory by the model of Chapman and Enskog:

$$\mu_l = 2.67 \times 10^{-6}\left(\frac{\sqrt{MT}}{\sigma^2 \Omega_\mu} \right) \tag{9}$$

where σ and Ω_μ are the Lennard-Jones constant collision diameter and the function collision integral respectively.
Turbulent viscosity is calculated according to the $k-\varepsilon$ model:

$$\mu_t = \rho C_\mu \frac{k^2}{\varepsilon} \tag{10}$$

The values of k and ε are calculated from the turbulent kinetic energy and turbulent dissipation rate equations:

DOI: 10.13009/EUCASS2017-268

$$\frac{\partial}{\partial t}(\rho k)+\frac{\partial}{\partial x_i}(\rho k u_i)=\frac{\partial}{\partial x_j}\left[\left(\mu+\frac{\mu_t}{\sigma_k}\right)\frac{\partial k}{\partial x_j}\right]+G_k-\rho\varepsilon-Y_M$$
$$\frac{\partial}{\partial t}(\rho \varepsilon)+\frac{\partial}{\partial x_i}(\rho \varepsilon u_i)=\frac{\partial}{\partial x_j}\left[\left(\mu+\frac{\mu_t}{\sigma_\varepsilon}\right)\frac{\partial \varepsilon}{\partial x_j}\right]+C_{1\varepsilon}\frac{\varepsilon}{k}G_k-C_{2\varepsilon}\rho\frac{\varepsilon^2}{k} \quad (11)$$

where σ_k and σ_ε are turbulent Prandtl number for k and ε. G_k is the source of turbulent kinetic energy due to velocity gradient, C_μ, $C_{1\varepsilon}$ and $C_{2\varepsilon}$ are model constants and Y_M is the turbulent kinetic energy sink due to density change.
The kerosene – oxygen reaction is assumed to be one-directional and neglects the existence of free radicals:

$$C_{12}H_{23}+17.75O_2\rightarrow 12CO_2+11.5H_2O \quad (12)$$

The reaction rate $R_{i,r}$ (Eq. 6) is controlled by either turbulent mixing or chemical kinetics. The smallest calculated value between the two mechanisms (Eq. (13-14) and Eq. (15)) is the one that determines the local reaction rate. It is calculated that way in order to prevent ignition before flame stabilizers.
The reaction rate based on the finite rate, eddy dissipation model is calculated from Eq. (13-14) where the smallest value of the two forms is considered.

$$R_{i,r}=\upsilon'_{i,r}M_{w,i}A\rho\frac{\varepsilon}{k}\min_R\left(\frac{Y_R}{\upsilon'_{R,r}M_{w,R}}\right) \quad (13)$$

$$R_{i,r}=\upsilon'_{i,r}M_{w,i}AB\rho\frac{\varepsilon}{k}\frac{\sum_p Y_p}{\sum_j^N \upsilon''_{R,r}M_{w,j}} \quad (14)$$

Where $\upsilon'_{i,r}$ and $\upsilon''_{i,r}$ are stoichiometric coefficient for reactant/products, Y_p is products mass fraction, Y_R is mass fraction of a specific reactant, A and B are model constants equal to 0.5 and 4 respectively.
The reaction rate considering chemical kinetics is given by the Arrhenius equation:

$$R_{i,r}=(\upsilon''_{i,r}-\upsilon'_{i,r})\left(k_{f,r}\prod_{j=1}^{N}\left[C_{j,r}\right]^{(\eta'_{j,r})}\right) \quad (15)$$

where $k_{f,r}$ is given by:

$$k_{f,r}=A_r T^{\beta_r-E_r/RT} \quad (16)$$

where $C_{j,r}$ molar concentration of the species j in the reaction, A_r is a constant and E_r is reaction activation energy.
The interaction between the injected kerosene/boron particles to the continuous flow-field is considered and the path of each injected particle is calculated in addition to mass and heat transfer. The solution is accomplished using the Euler-Lagrange method for continuous flow-field and the Navier-Stokes equations are solved with the addition of the discrete particles. Collision of the kerosene droplets is modeled by O'Rourke model, which assumes stochastic collision between the droplets. Droplet breakup is modeled by Reitz wave model. Particle track prediction is obtained according to:

$$\frac{du_p}{dt}=F_D(u-u_p)+F_x \quad (17)$$

DOI: 10.13009/EUCASS2017-268

where the droplet drag force F_D is given by:

$$F_D = \frac{18\mu}{\rho_P d_P^2}\frac{C_D \,\mathrm{Re}}{24} \tag{18}$$

The particle properties vary according to its temperature. When the particle temperature is lower than its evaporation temperature, its temperature is calculated according to inert heat/cooling equation:

$$T_P(t+\Delta t) = T_\infty + \left[T_P(t) - T_\infty\right] e^{-A_p h / m_p c_P \cdot \Delta t} \tag{19}$$

where the convection coefficient h is calculated using the correlation for Nusselt number described by:

$$Nu = \frac{h d_p}{k_\infty} = 2 + 0.6\,\mathrm{Re}_d^{1/2}\,\mathrm{Pr}^{1/3} \tag{20}$$

where Re_d is the Reynolds number and Pr is the Prandtl number calculated according to the particle diameter and the relative velocity between the flow-field and the particle. At the point that the particle temperature reaches its evaporation temperature the particle evaporation model is used. It is assumed that the particle evaporation rate is governed by the concentration gradient from the discrete to continuous phase and is determined by the difference between the particle vapor pressure and bulk pressure. The vapor molar flux is given by:

$$N_i = K_c(C_{i,s} - C_{i,\infty}) \tag{21}$$

where $C_{i,s}$ is the vapor concentration on the particle surface, described by Eq. (22), $C_{i,\infty}$ is the vapor concentration of the bulk flow, described by Eq. (23) and K_c is the mass flow coefficient, given by Eq. (24).

$$C_{i,s} = \frac{P_{sat}(T_p)}{RT_p} \tag{22}$$

$$C_{i,\infty} = X_i \frac{p}{RT_\infty} \tag{23}$$

$$K_c = \frac{D_{i,m}}{d_p}\left(2 + 0.6\,\mathrm{Re}_d^{1/2}\,Sc^{1/3}\right) \tag{24}$$

The droplet saturation pressure $p_{sat}(T_P)$ is calculated as a function of the droplet temperature for a liquid state droplet. As regards a gel droplet, the saturation pressure is calculated as a function of temperature and the droplet time-cycle that takes into account the periodic vaporization and is given by:

$$\begin{aligned} t_p < 1.5ms &\rightarrow p_{sat} = p\cdot(1+\cos\omega t)/2 \\ t_p > 1.5ms &\rightarrow p_{sat} = p\cdot(1+\cos\omega t) \end{aligned} \tag{25}$$

where ω is the gel droplet evaporation frequency. A transient period of $t = 1.5ms$ is chosen in order to smooth the droplet saturation pressure value.
Droplet mass is reduced according to Eq. (26) and its temperature is determined according to Eq. (27):

$$m_p(t+\Delta t) = m_p(t) - N_i A_p M_{w,i} \Delta t \tag{26}$$

DOI: 10.13009/EUCASS2017-268

$$m_p c_p \frac{dT_p}{dt} = hA_p(T_\infty - T_p) + \frac{dm_p}{dt} h_{fg} \tag{27}$$

where h_{fg} is droplet latent heat.

When droplet temperature reaches boiling temperature, the vaporization rate is determined by the d^2 law. In this case, the droplet temperature is its boiling temperature and the droplet diameter is calculated according to Eq. (28). All the other droplet properties are calculated according to Eqs. (21)-(27).

$$\frac{d(d_p)}{dt} = \frac{4k_\infty}{\rho_p c_{p,\infty} d_p}(1 + 0.23\sqrt{\mathrm{Re}_d}) \ln\left[1 + \frac{c_{p,\infty}(T_\infty - T_p)}{h_{fg}}\right] \tag{28}$$

Boron ignition and combustion has been modelled using King's model[3].

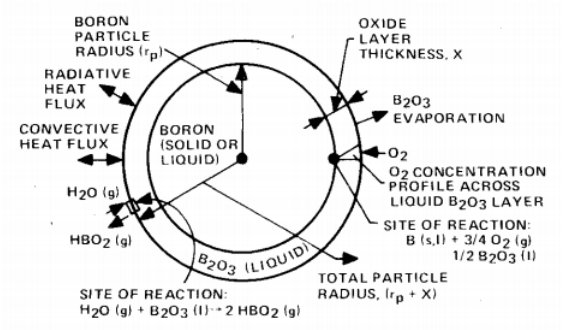

Figure 3. Schematic of boron particle combustion process [3].

The model divides the combustion of the boron into two stages. The first stage is the ignition stage in which the boron particles are covered by a boron-oxide thin layer that prevents from ambient oxygen to reach the boron core and react. Typical oxide layer thickness is 0.1 μ - 0.2 μ. At this stage, boron particle diameter change is calculated according to Eq. 29:

$$\frac{d(d_B)}{dt} = -\frac{2R_B M_B}{\pi {d_B}^2 \rho_B} \tag{29}$$

where R_B is boron consumption rate.

$$R_B = 0.16\times10^{-12} {d_p}^2 T_p X_{O_2} p / \delta e^{-22600/T_P} \tag{30}$$

where δ is boron oxide thickness. The expression is based on experimental results of Talley and Henderson [7] and consistent with King's model [3].
Boron-oxide thickness change is calculated according to:

$$\frac{d(\delta)}{dt} = -\frac{(R_B/2 - R_E - R_H) M_{B_2O_2}}{\pi {d_B}^2 \rho_{B_2O_2}} \tag{31}$$

Where R_E is boron-oxide evaporation rate and R_H is the reaction rate with vapor, the expressions for the rates are:

$$R_E = \frac{0.32\times10^9 \pi {d_p}^2 (Nu) {T_P}^{1/2}}{T_P(Nu) + 887 p d_P} e^{-44000/T_P} \tag{32}$$

DOI: 10.13009/EUCASS2017-268

$$R_H = 4.575\times10^{-3}\frac{Nu}{p}d_P T_P^{1/2}\exp[18.1(1-2100/T_P)]\cdot \\ \cdot[-0.15+\{0.0225+0.987X_{H_2O}p\exp[18.1(1-2100/T_P)\}^{0.5}] \tag{33}$$

Particle temperature change rate is calculated from energy conservation:

$$\frac{dT_P}{dt} = -\frac{\dot{Q}_{TOT}}{\frac{\pi}{6}d_B{}^3 c_{pB}\rho_B + \pi d_B{}^2\delta c_{pB_2O_3}\rho_{B_2O_3}} \tag{34}$$

where $\dot{Q}_{TOT}$ is the sum of the heat rates caused by radiation, conduction, evaporation and the chemical reactions.
At 2450K boron is starting to melt. The rate of melting is expressed by:

$$\frac{df_M}{dt} = -\frac{\dot{Q}_{TOT}}{\frac{\pi}{6}d_B{}^3\rho_B\Delta H_M} \tag{35}$$

While at this stage the temperature of the particle is kept constant and the temperature continue to rise after the melting stage is completed.
The ignition stage is over when boron-oxide is completely removed from the particle, and then, the combustion stage begins, the rate of diameter changes is:

$$\frac{d(d_B)}{dt} = -4\frac{\rho_g D}{\rho_B d_B}\ln(1+B) \tag{36}$$

Where D is the gas diffusivity and B is the Spalding number expressed by:

$$B = \frac{\xi y_{O_2,\infty} + y_{B,S}}{1-y_{B,S}} \tag{37}$$

ξ is the stoichiometric ratio derived from the reaction:

$$B + \tfrac{3}{4}O_2 \rightarrow \tfrac{1}{2}B_2O_3 \tag{38}$$

Equations 32-38 are calculated in each time step of the discrete phase module.

3. Numerical Solution

As mentioned, the programing and numerical solving we use in the study is FLUENT CFD code [6]. Firstly, the flowfield was meshed in $2\cdot10^6$ computational cells, whereas the boundary layer and flame stabilizers zone mesh were further refined. Then, each of the governing equations: continuity, momentum conservation, energy, turbulence and chemical species is solved in each cell until convergence is reached.
A pressure-based coupled solver was chosen as the solution scheme. In this scheme, the velocity field is calculated from the pressure equation as the pressure equation is derived from the continuity and momentum conservation equations. The velocity field was updated by the calculated pressure. The energy, turbulence and chemical species were calculated using the updated flowfield properties and the flowfield was updated due to interaction with the discrete particles. Finally, the residual was calculated. Because of the complexity of solving combusting flowfield, the solution is divided to several steps and the solution of each step serves as the initial condition for the next step. First, the cold flowfield through-out the combusting chamber is solved including the mass, momentum, energy and turbulence equations. Next, inert droplets are injected. After convergence, the droplets are defined as kerosene droplets and finally the reaction scheme is enabled and the combustor is ignited.

DOI: 10.13009/EUCASS2017-268

Boron particles are at first injected as inert and after stabilization of the flowfield their combustion is defined by UDF (User Defined Function), which simulates the two stages. Finally, the flowfield is solved iteratively until convergence to the defined residual is achieved. Droplet size was normally distributed between 10-50 microns with mean diameter of 23 microns. For the boron combustion, the metalized particles were injected separately from the gel kerosene droplets in the following method. Theoretically, the boron particles are uncovered after the evaporation of the kerosene. Examining the flowfield one can see that large number of droplets are vaporized in the zone after the flame holders; therefore, boron particles are injected discretely at that point. The initial temperature of the particles is the local temperature at the injection point.

4. Results

The scope of the present research is to investigate the effect of various parameters, such as the bypass ratio, the boron content, the particle diameter distribution etc.; however in the present paper just the initial results are presented to demonstrate the validity of the model and the numerical solution.
Figure 4 presents the temperature field in the combustor. It can be seen that initial hydrocarbon-air combustion occurs downstream the fuel injection, the temperature rises and falls slightly when the particles are “injected” further downstream. Then, temperature rises again and decreases significantly in the vicinity of the bypass air introduction. The additional air promotes combustion and when the flow accelerates close to the nozzle, temperature decreases. As expected, temperature decreases in the expansion in the nozzle.

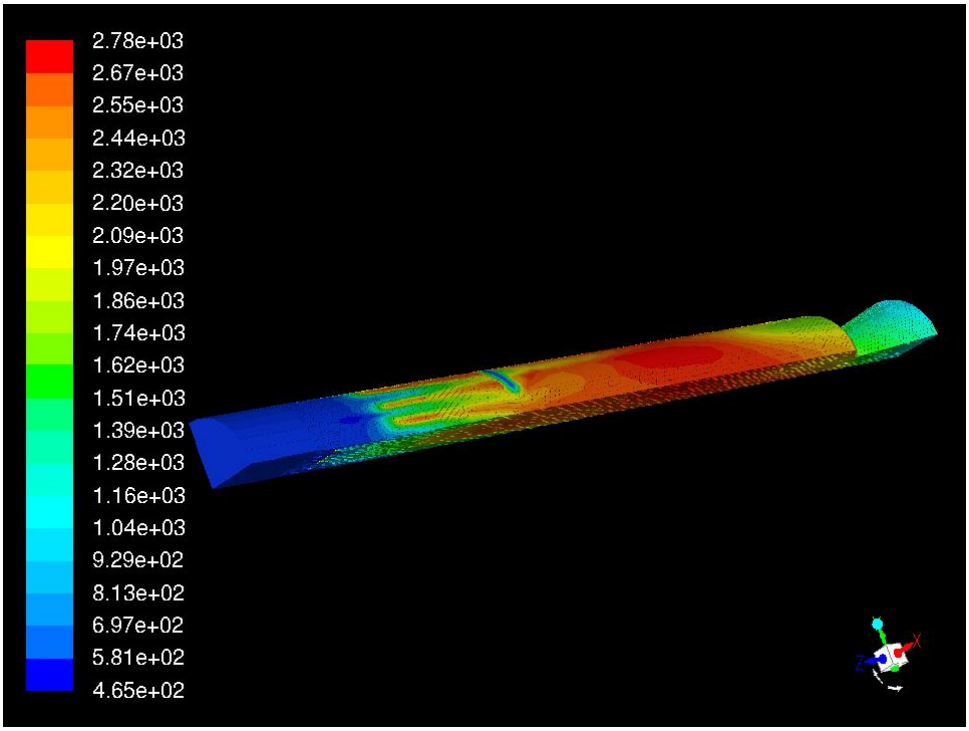

Figure 4. Temperature field in the combustor [K]

The Mach number inside the combustor is presented in Fig. 5. As expected, the flow is subsonic and becomes supersonic only after the nozzle throat.
The average boron particle diameter distribution is presented in Fig. 6. As shown, the particle diameter decreases as we move downstream.

DOI: 10.13009/EUCASS2017-268

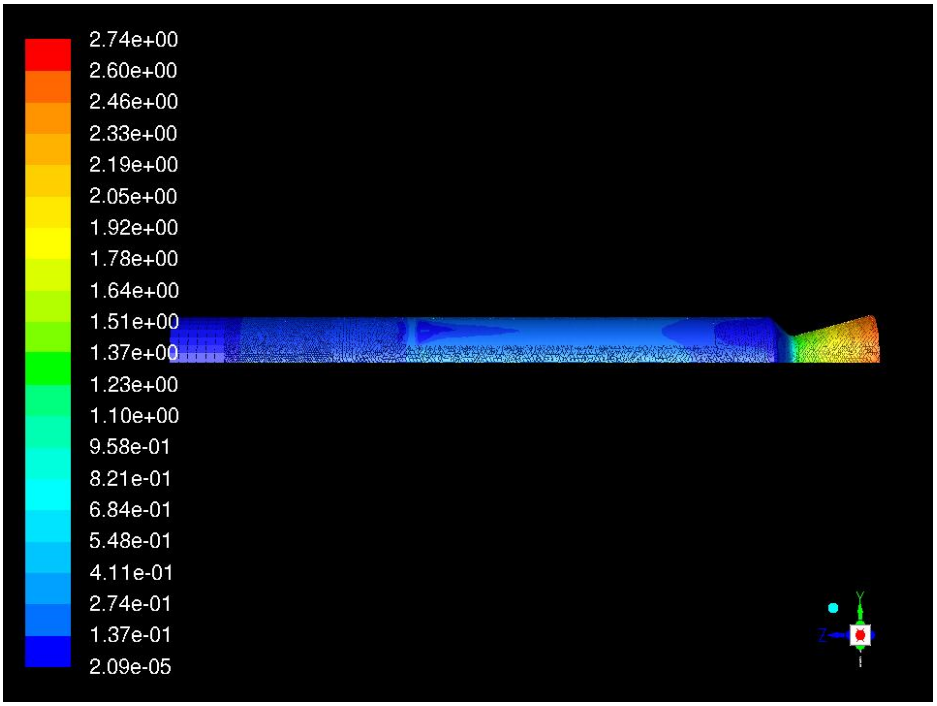

Figure 5. Mach number in the combustor

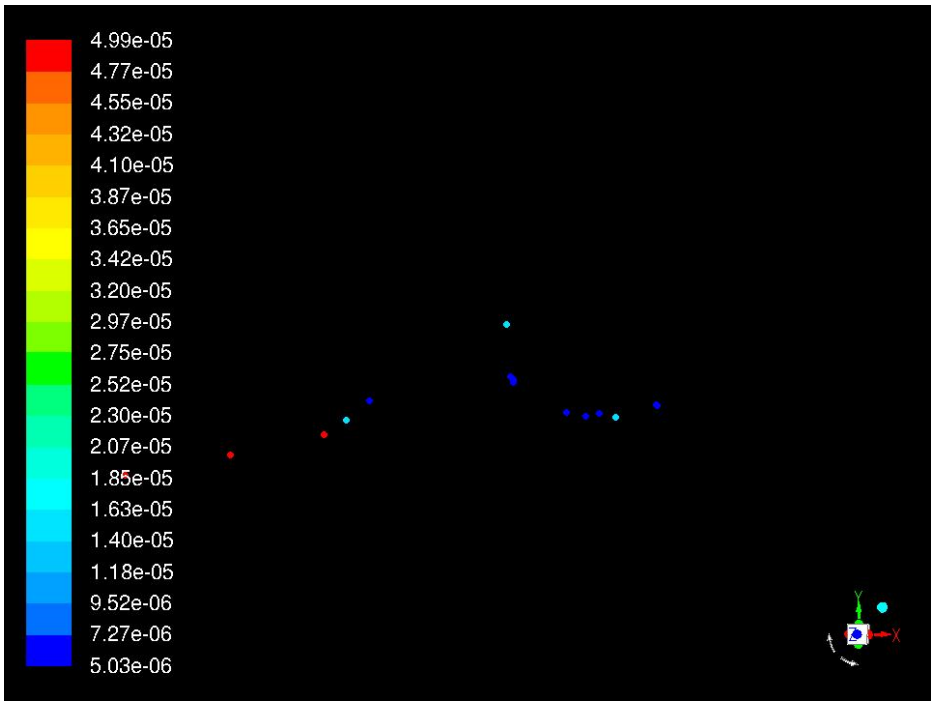

Figure 6. Boron particle diameter in the combustor [μ]

From these partial results, it can be interpreted that boron particles ignite and burn in the flowfield.

5. Conclusions

In the present study a theoretical model for the flowfield of a boron-loaded gel fuel ramjet was developed and solved numerically. The results indicate the validity of the model.

DOI: 10.13009/EUCASS2017-268

References

[1] Fry, R. S. 2004. A century of ramjet propulsion technology evolution. *J. Propuls. Power*, 20:27-58.
[2] Haddad, A., Natan, B. and Arieli, R. 2011. The Performance of a boron loaded gel fuel ramjet. In *Progress in Propulsion Physics*. 2:549-568.
[3] King, M.K. 1982. Ignition and combustion of boron particles and clouds. *J. Spacecr. Rockets*. 19:294-300.
[4] Natan, B. and Gany, A. 1993. Effects of bypass air on boron combustion in solid fuel ramjets. *J. Propuls. Power*. 9:155-157.
[5] Matsibeker E., and Natan, B. 2013. Numerical solution of the flowfield in an aluminized gel fuel ramjet. AIAA paper 2013-3976.
[6] ANSYS FLUENT Theory guide, Release 17.2, August 2016 .
[7] Talley, C.P and Henderson, U.V. 1961. Combustion of elemental boron. In 4th meeting JANAF-ARPA-NASA Thermochemical panel. 107-121.